Kobe University Repository : Kernel

PDF issue: 2025-12-04

Fluorescent Signaling of Molecularly Imprinted Nanogels Prepared via Postimprinting Modifications for Specific Protein Detection

Tsutsumi, Katsuki ; Sunayama, Hirobumi ; Kitayama, Yukiya ; Takano, Eri ; Nakamachi, Yuji ; Sasaki, Ryohei ; Takeuchi, Toshifumi

(Citation)
Advanced NanoBiomed Research,1(4):2000079

(Issue Date)
2021-02-08

(Resource Type)
journal article

(Version)
Version of Record

(Rights)
© 2021 The Authors. Advanced NanoBiomed Research published by Wiley-VCH GmbH.
This is an open access article under the terms of the Creative Commons Attribution License, which permits use, distribution and reproduction in any medium, provided the original work is properly cited.

(URL)
https://hdl.handle.net/20.500.14094/90009488

ADVANCED NANOBIOMED RESEARCH
www.advnanobiomedres.com

Fluorescent Signaling of Molecularly Imprinted Nanogels Prepared via Postimprinting Modifications for Specific Protein Detection

*Katsuki Tsutsumi, Hirobumi Sunayama, Yukiya Kitayama, Eri Takano, Yuji Nakamachi, Ryohei Sasaki, and Toshifumi Takeuchi**

Previous reports have stated the advantages of postimprinting modification (PIM) to develop multifunctional molecularly imprinted polymers (MIPs). However, existing technologies have only been applied on bulk- and film-based MIPs. Herein, the fluorescent signaling of nanogels (NGs) for protein detection is demonstrated. The NGs are prepared by molecular imprinting and PIM. A bivalent functional monomer, 4-[2-(*N*-methacrylamido)ethylaminomethyl] benzoic acid (FM1), comprising a benzoic acid moiety for interaction with proteins and secondary amine group for incorporating fluorescent reporter molecules is used. Human serum albumin (HSA), a marker protein for human health, serves as the model protein. HSA-imprinted NGs (MIP-NGs) are prepared by emulsifier-free precipitation polymerization of FM1, *N*-isopropylacrylamide, 2-methacryloxyethyl phosphorylcholine, and *N,N′*-methylenebis acrylamide in the presence of HSA. After the removal of HSA, a fluorescent dye (ATTO 647 N) is treated with amino groups on FM1 residue as the PIM; this yields fluorescent-signaling MIP-NGs (FL-MIP-NGs) of ≈20 nm in diameter. The FL-MIP-NG-based sensing system detects HSA in a real sample by selectively reading out the HSA-binding events as high-affinity fluorescence changes ($K_d = 2.5 \times 10^{-9}$ M). The proposed MIP-NGs functionalized via PIMs serve as advanced functional materials for sensing biorelated compounds.

1. Introduction

Functional materials capable of specific molecular recognition are of great importance in fields such as life sciences and medicine. Antibodies are frequently used in these fields as a molecular recognition element because of their high affinity and selectivity toward target molecules. Antibodies have been deemed as attractive for use in various applications such as biosensing, imaging of biorelated compounds,[1] therapeutics, and diagnosis.[2–4] However, antibodies have some drawbacks, including high production costs, tedious detection procedures, and low stabilities with regard to chemical/physical stimuli. Therefore, alternatives that overcome these drawbacks are required. Several efforts have been made to develop synthetic materials that are capable of molecular recognition based on peptides,[5] oligo-DNAs,[6,7] and synthetic polymers.[8,9]

Molecularly imprinted polymers (MIPs) are potential alternatives for antibodies because they are easy to prepare, exhibit high stabilities, and are applicable to various molecules.[10–13] Conventional MIPs are prepared by radical polymerization of functional monomers, which are capable of interaction with a target molecule, comonomers, and crosslinkers in the presence of the target molecule. After the removal of the template molecules, molecularly imprinted cavities having a complementary shape and size to the target molecule are created in the polymer matrix. Various approaches involving covalent imprinting[14] for creating MIPs with specific molecular

K. Tsutsumi, Dr. H. Sunayama, Dr. Y. Kitayama, Dr. E. Takano, Prof. T. Takeuchi
Graduate School of Engineering
Kobe University
1-1, Rokkodai-cho, Nada-ku, Kobe 657-8501, Japan
E-mail: takeuchi@gold.kobe-u.ac.jp

The ORCID identification number(s) for the author(s) of this article can be found under https://doi.org/10.1002/anbr.202000079.

© 2021 The Authors. Advanced NanoBiomed Research published by Wiley-VCH GmbH. This is an open access article under the terms of the Creative Commons Attribution License, which permits use, distribution and reproduction in any medium, provided the original work is properly cited.

DOI: 10.1002/anbr.202000079

Dr. Y. Nakamachi
Department of Clinical Laboratory
Kobe University Hospital
7-5-2 Kusunoki-cho, Chuo-ku, Kobe 650-0017, Japan

Prof. R. Sasaki
Division of Radiation Oncology
Kobe University Hospital
7-5-2 Kusunoki-cho, Chuo-ku, Kobe 650-0017, Japan

Prof. R. Sasaki, Prof. T. Takeuchi
Center for Advanced Medical Engineering Research & Development (CAMED)
Kobe University
1-5-1 Minatojimaminami-machi, Chuo-ku, Kobe 650-0047, Japan

recognition ability have been established, such as surface imprinting[15] and oriented immobilization using specific ligands.[16–18] However, only a few recent publications have reported MIPs with affinities high enough to be comparable with natural antibodies. The only function of MIPs is to selectively capture molecules according to their preparation procedure, making it difficult for them to perform other functions such as signaling. Conventionally, multifunctional monomers that incorporate additional functional groups, such as fluorescent dye moiety,[19,20] photoresponsive moiety,[21,22] or catalytic moiety,[23,24] have been used to manufacture multifunctional MIPs. However, the random incorporation of these monomer residues into the MIP matrix could induce undesired nonspecific expressions of their function.

Postimprinting modification (PIM) is an attractive strategy to develop multifunctional MIPs, which allows site-specific introduction of various functional groups into the imprinted cavity after construction of MIPs.[25] The aforementioned examples are the demonstrations of the fabrication of various multifunctional MIPs via PIMs, which involve exchanging the interaction groups that lead to a regulation of the binding activity of the MIP[26–28] and cause fluorescent dye conjugation for the formation of fluorescent-signaling MIPs with high signal-to-noise (S/N) ratio.[29–31] These PIM technologies have only been applied on bulk- and film-based MIPs.[25] Therefore, producing a nanoparticle-based MIP that is functionalized by PIMs is still challenging. Nanosized materials are used for a wide range of purposes including in vitro/in vivo imaging, drug delivery for disease treatment, and therapeutics.[32,33] The development of MIP nanoparticles functionalized by PIM could extend the range of applications of MIP-based materials.[34]

In this study, the fluorescent-signaling MIP nanogels (FL-MIP-NGs) that are used for specific protein detection have been prepared by emulsifier-free precipitation polymerization and molecular imprinting with a functional monomer 4-[2-(*N*-methacrylamido)ethylaminomethyl] benzoic acid (FM1); this monomer comprises a benzoic acid moiety for interaction with the target protein and a secondary amino group for the incorporation of the fluorescent reporter dye as a PIM (**Figure 1**).[35] Human serum albumin (HSA), which is abundant in human serum and a biomarker for human healthcare including certain hepatic diseases, inflammation, malnutrition, nephritic syndrome, and uremia,[36–38] was used as a model target protein. We examined the protein-binding properties and fluorescent-signaling ability of the prepared FL-MIP-NGs using a surface plasmon resonance (SPR) sensing system and fluorescence microscope measurements.

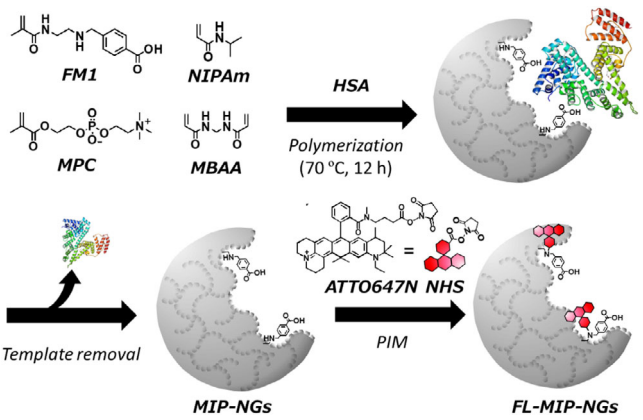

Figure 1. Schematic illustration of the preparation of FL-MIP-NGs by molecular imprinting and PIM.

2. Results and Discussion

2.1. Preparation of HSA-Imprinted Polymer NGs

HSA-imprinted NGs (MIP-NGs) were prepared via emulsifier-free precipitation polymerization in a 10 mM phosphate buffer (pH 7.4, with 140 mM NaCl) at 70 °C for 12 h. Under the polymerization conditions, the secondary structure of HSA was maintained as previously reported.[33] The following compounds were polymerized in the presence of HSA: FM1 possessing benzoic acid that was added for interaction with the amino acid residues on HSA, NIPAm that was incorporated as the main component, MPC that was added as a comonomer for achieving high biocompatibility,[39] and MBAA that was incorporated as a hydrophilic crosslinker (Figure 1). As a reference, NIP-NGs were also prepared identically to the MIP, except for HSA addition. The obtained NGs were purified by size-exclusive chromatography; subsequently, anion-exchange chromatography was conducted to remove the residual monomer and template HSA. The obtained chromatograms indicated that the NGs were successfully purified and removed from the template HSA (Figure S1, Supporting Information). Purified NGs were characterized by dynamic light scattering (DLS) measurement and their average diameters were estimated to be 18.0 nm for MIP and 13.7 nm for NIP (Figure S2, Supporting Information). The transmission electron microscope (TEM) images also indicated that nanometer-sized particles were observed (Figure S3, Supporting Information). These results indicated the successful synthesis of nanosized polymer gels. Since the size of precipitated polymer NGs depends on surface free energy between generated polymers and the solvent used, the size control would be possible by changing the hydrophobic/hydrophilic property of the monomers used.

We investigated the binding abilities of NGs toward HSA using a SPR sensing system. For this purpose, the prepared NGs were immobilized on the gold-coated substrate. MIP-NGs demonstrated a higher affinity toward the target protein (HSA) than that demonstrated by NIP-NGs (**Figure 2**). The dissociation constants (K_d) of the NGs were calculated using a curve-fitting software based on 1:1 binding model, for $K_d = 2.00 \times 10^{-8}$ M (MIP-NGs) and $K_d = 1.67 \times 10^{-7}$ M (NIP-NGs), respectively (Figure S6a and S6b, Supporting Information). The K_d value of MIP-NGs was 8.4 times lower than that of NIP-NGs. Therefore, this confirmed that the HSA-binding cavity was formed in the MIP-NG matrix during the molecular imprinting process.

2.2. PIM of the Prepared NGs and Their Protein-Binding Property

In PIMs, a fluorescent reporter molecule (ATTO 647 N) was introduced into the secondary amino groups that were present

© 2021 The Authors. Advanced NanoBiomed Research published by Wiley-VCH GmbH

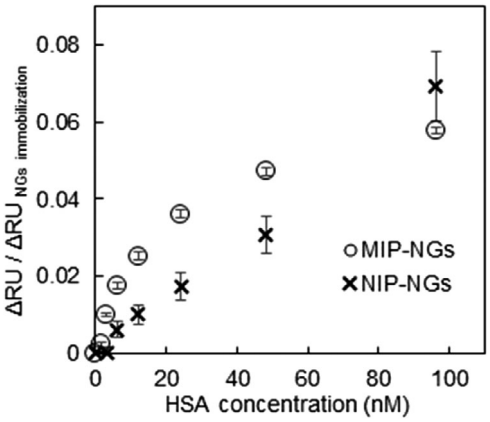

Figure 2. HSA binding isotherm of MIP-NGs and NIP-NGs evaluated by the SPR measurement. The error bars were calculated from quadruple experiments.

on the FM residues in the MIP matrix via NHS-mediated amine coupling, resulting in the formation of fluorescent-labeled MIP-NGs (FL-MIP-NGs). A characteristic fluorescent spectrum around 664 nm ($\lambda_{Ex} = 646$ nm) was observed after modification, confirming that the ATTO 647 N fluorescent dye was successfully incorporated into the MIP matrix (Figure S4, Supporting Information). Binding properties of FL-MIP-NGs were also examined by the SPR sensing system. Consequently, the HSA-binding ability of FL-MIP-NG was maintained even after the PIM treatment, resulting in the binding constant (K_d) of 3.15×10^{-9} M (**Figure 3**a and S6c, Supporting Information). We observed a slight increase in the binding affinity after PIMs. The introduction of a hydrophobic fluorescent dye (ATTO 647 N)[29] resulted in the formation of a hydrophobic microenvironment in the imprinted cavity, which is a factor that could be attributed to the increase in the interaction between MIP-NGs and HSA. As it is well known that the drug-binding site 1 on HSA can interact with a wide variety drugs, the hydrophobic ATTO 647 N structure may bind to this binding pocket,[40] resulting in an increase in the selective binding for HSA (Figure 3b). We also examined protein selectivity using transferrin (Trf; Mw: 80 kDa; p*I*: 5.8) and cytochrome c (Cyt; Mw: 12.4 kDa; p*I*: 10) as reference proteins. As shown in Figure 3b, SPR responses of FL-MIP-NGs toward HSA were higher than those of other proteins, indicating that the selective capture of HSA was achieved by FL-MIP-NGs.

2.3. Fluorescent-Signaling Ability of FL-MIP-NGs

The fluorescent-signaling ability of FL-MIP-NGs toward HSA was investigated using a custom-made fluorescence microscope equipped with a programmable liquid-handling robot (System Instruments Co. Ltd., Tokyo, Japan) (Figure S5, Supporting Information).[41,42] For easier handling of the prepared FL-MIP-NGs, the NGs were immobilized on a gold-coated glass substrate and put in a custom-made flat-type pipette chip (Figure S5, Supporting Information). The intensity of immobilized FL-MIP-NGs was recorded with a cMOS camera equipped with a fluorescence microscope. The relative fluorescent changes ($(F - F_0)/F_0$), with each addition of HSA, were calculated. F_0 is the fluorescence intensity in 10 mM phosphate buffer (pH 7.4, 140 mM NaCl), and F is the fluorescence intensity in an HSA sample dissolved in the phosphate buffer. The FL-MIP-NGs fluorescence was increased by increasing the HSA concentration (**Figure 4**a).

The fluorescence change of MIP was greater than that of NIP, indicating the formation of the HSA-binding cavity that comprised the ATTO dye in the MIP matrix. The apparent binding constant (K_d) was estimated to be 2.50×10^{-9} M (Figure S6d, Supporting Information) from the given binding isotherm, which is similar to the value calculated from SPR measurements. Therefore, this implies that fluorescent changes were caused by HSA binding. We achieved sensitive and selective detection of HSA in the linear range of 12–192 nM, with a detection limit of 13 nM (Figure S7, Supporting Information). This sensitivity is slightly lower than the previously reported values when antibodies were used as a molecular recognition element,[43] and that is higher or comparable with previously developed MIP-based fluorescent sensors toward HSA.[19,44,45]

The observed increase in fluorescence intensity may be due to the stabilization of the fluorescent dye molecule by HSA binding

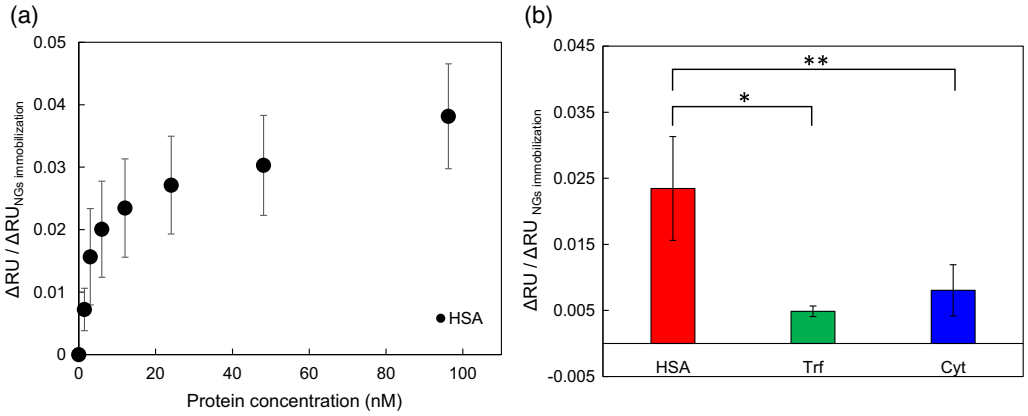

Figure 3. a) HSA binding isotherms of FL-MIP-NGs evaluated by SPR measurements. b) A selectivity test of FL-MIP-NGs using HSA, transferrin (Trf), and cytochrome c (Cyt) (protein concentration, 12 nM). The error bars were calculated from quadruple experiments (* = 0.021, ** = 0.0016).

© 2021 The Authors. Advanced NanoBiomed Research published by Wiley-VCH GmbH

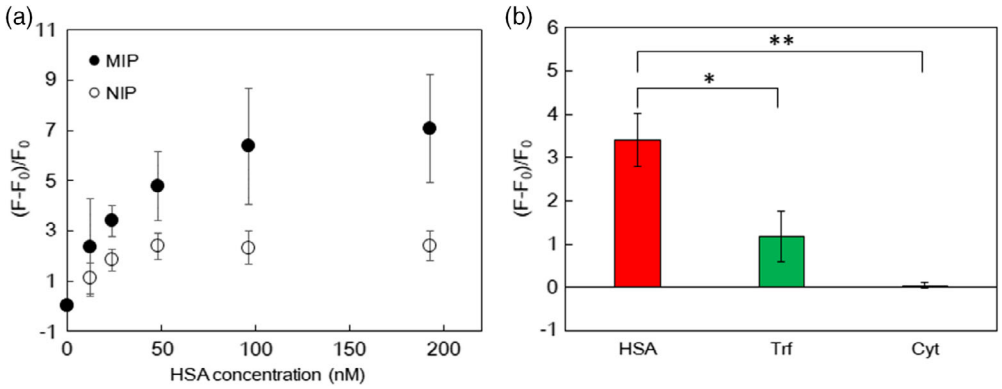

Figure 4. a) HSA binding isotherms of FL-MIP-NGs and FL-NIP-NGs evaluated by fluorescent measurements. b) Selectivity test of FL-MIP-NGs using HSA, transferrin (Trf), and cytochrome c (Cyt) (protein concentration: 24 nM). The error bars were calculated from triplicate experiments (* = 0.0065, ** = 0.023).

and/or due to the microenvironment for becoming more hydrophobic around the fluorescent dye, as fluorescence intensity of ATTO 647 N increased in the organic solvent (dichloromethane) (Figure S8, Supporting Information). The selectivity of FL-MIP-NGs was examined using the reference proteins, Trf and Cyt (Figure 4b). We observed little or no response in the relative fluorescence change when the reference proteins were examined, confirming the selective HSA detection by fluorescence. The FL-MIP-NG fluorescent measurements demonstrated more HSA selectivity than that demonstrated by the SPR measurements. This was due to a difference in the detection principle between the two measurements. The fluorescent change was caused by a microenvironmental change around the fluorescent dye whereas the SPR response was caused by reflective index changes that occurred near the metal surfaces. Consequently, fluorescent measurements indicated a binding event that occurred around the fluorescent dye, whereas the SPR response reflected the total binding on the substrate surface. We observed an increased degree of HSA-selective detection in fluorescence, indicating that the fluorescent dye ATTO 647 N was selectively introduced into the imprinted cavity during PIMs.

The behavior of fluorescent response toward Trf appeared to be different from that of Cyt; the selectivity for Trf in the fluorescence measurements was not significantly improved. The fluorescence response is principally derived from their interaction with the fluorescence dye. Thus, larger Trf (Mw: 80 kDa and p*I*: 5.8) could affect the fluorescence response more than smaller Cyt (Mw: 12.4 kDa, p*I*: 10), even for smaller amounts of nonspecifically bound Trf. Furthermore, as the dye was positively charged under binding conditions, an acidic protein Trf may interact with the fluorescence dye more easily than basic protein Cyt. Therefore, the selectivity for Trf was observed to be less improved than that of Cyt. However, such undesirable PIM sites in incomplete imprinted cavities can be hindered before introducing the fluorescence dye by a previously reported multistep PIM, called a capping treatment.[35,46]

We also observed the fluorescent-signaling ability of FL-MIP-NGs in a diluted clinical serum sample. Clinical serum samples were collected from patient volunteers in Kobe University Hospital ($n = 8$). Informed consent of all participants was obtained as per the guidelines of the Institutional Review Board in Kobe University Hospital (#180128) and the Graduate School of Engineering, Kobe University (#30-03). The serum samples were diluted 10 000 times using a 10 mM phosphate buffer of pH 7.4 containing 140 mM NaCl; this was aimed at adjusting the albumin concentration to the available dynamic range of the FL-MIP-NGs sensing chip. The HSA concentration in the serum was estimated by the conventional bromocresol purple (BCP) method, which has been frequently used for quantification of HSA in clinical samples (Table S1, Supporting Information). The BCP method is based on the HSA-selective adsorption property of bromocresol purple.[38] **Figure 5** shows a good correlation between fluorescent detection by FL-MIP-NGs and the conventional BCP method. This proof-of-concept test shows that the prepared FL-MIP-NG-based sensing system has the potential to selectively read out HSA-binding events in diluted serum samples.

3. Conclusions

We have prepared MIP-NGs by the emulsifier-free precipitation polymerization of FM1, NIPAm, MPC, and MBAA in the

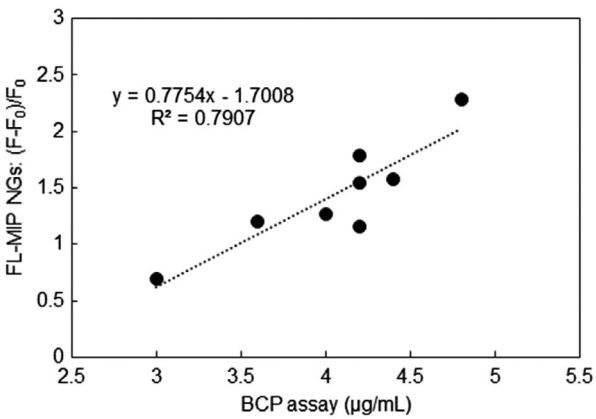

Figure 5. Comparison of the proposed FL-MIP-NG-based sensing system and the conventional BCP method.

© 2021 The Authors. Advanced NanoBiomed Research published by Wiley-VCH GmbH

presence of HSA and a fluorescent dye with FM1 residue. This was aimed at producing fluorescent-signaling MIP-NGs (FL-MIP-NGs). The fluorescent response of FL-MIP-NGs toward proteins was examined using a fluorescence microscope in a custom-made liquid-handling robot. The FL-MIP-NGs-based sensor showed a high affinity ($K_d = 10^{-9}$ order) and low cross-reactivity. Our investigation on the protein-binding processes of FL-MIP-NGs by fluorescence and SPR measurements revealed that the selective introduction of a fluorescence dye near the interaction site as a PIM suppresses the fluorescent signal from the nonspecific binding of off-target proteins. Furthermore, the FL-MIP-NGs-based sensor showed the potential to detect HSA in clinical samples with high sensitivity and selectivity. Therefore, we believe that signaling MIP-NGs that have been functionalized using PIMs provide a promising way of developing advanced materials for sensing and imaging of biorelevant molecules that can be effectively used in therapeutics and diagnosis.

4. Experimental Section

Materials: Ethanol (EtOH), sodium dihydrogen phosphate, disodium hydrogen phosphate, sodium chloride (NaCl), dimethyl sulfoxide (DMSO), sodium dodecyl sulfate (SDS), 2,2′-azobis(2-methylpropioamidine), dihydrochloride (V-50), 2-amino ethanol, transferrin (HOLO) from human blood (Trf), and HSA were purchased from Wako Pure Chemical Co. Ltd (Osaka, Japan). 1-ethyl-3-(3-dimethylaminopropyl) carbodiimide hydrochloride (EDC) was purchased from Tokyo Chemical Industries (Tokyo, Japan). *N*-Isopropyl acrylamide (NIPAm), *N,N′*-methylenebisacrylamide (MBAA), and cytochrome c (Cyt) were purchased from Nacalai Tesque Co. (Kyoto, Japan). DEDA-Sephadex, *N*-hydroxysuccinimide (NHS), and 11-mercaptoundecanoic acid were purchased from Sigma-Aldrich (MO, USA). ATTO 647 N NHS ester was purchased from ATTO-TEC GmbH (Siegen, Germany). 2-Methacryloyloxyethyl phosphorylcholine (MPC) was purchased from NOF Corporation (Tokyo, Japan). The water used in all experiments was obtained from a Millipore Milli-Q purification system. The Au-coated SPR sensor chips (superficial area: 120 mm^2) were purchased from GE Healthcare Japan (Tokyo, Japan). The functional monomer, 4-[2-(*N*-methacrylamido)ethylaminomethyl] benzoic acid (FM1), was synthesized according to the previously reported procedure.[35,47]

Characterization: DLS measurements were carried out using Zetasizer Nano ZS (Malvern Instruments Ltd., UK). SPR measurements were carried out using a Biacore 3000 instrument (GE Healthcare Japan). The fluorescence microscopy measurements were carried out with an automatic analyzing device, including a tip rack, reagent rack, an incubation port, and computer (System Instruments Co. Ltd., Japan). For the automatic analyzer, a pipette tip suitable for mounting a gold-coated glass substrate (4.3 × 9.8 mm) was designed and set in the chip rack. This automatic analyzing system was demonstrated using a device capable of pipetting, incubating, washing, and detecting, according to the program's input in the computer.[41,48] BCP assay was conducted using a clinical biochemistry analyzer JCA-BM8040G (JEOL Ltd., Tokyo, Japan).

Preparation of Polymer Nanoparticles (MIP-NGs and NIP-NGs): HSA (6.70 mg, 0.1 μmol), FM1 (39.3 mg, 0.150 mmol), NIPAm (204 mg, 1.81 mmol), MPC (29.5 mg, 0.100 mmol), MBAA (16.5 mg, 0.108 mmol), and V-50 (109 mg, 0.400 mmol) were dissolved in 10 mM phosphate buffer (pH 7.4, containing 140 mM NaCl) and incubated for 24 h at 4 °C. The mixture was placed in a Schlenk flask, and emulsifier-free precipitation polymerization was conducted in nitrogen atmosphere for 12 h at 70 °C. After polymerization, residual monomer species were removed by ultrafiltration (25 °C, 7500 g, 20 min × 3) using a centrifugal filter unit (Amicon Ultra 4–10 kDa, Merk, USA) and simultaneously exchanged the solvent to 10 mM Tris-HCl buffer (pH 7.4, 140 mM NaCl). The solution (1.0 mL) was applied to the column packed with the anion-exchange resin (DEAE-Sephadex) and eluted by 10 mM Tris-HCl buffer (pH 7.4, 140 mM NaCl). The elution was collected for each 1.5 mL fraction and examined for fluorescence at 340 and 400 nm ($\lambda_{ex} = 280$ nm each) derived from HSA and FM1, respectively. Only the fractions with fluorescence at 400 nm derived from FM1 were observed, combined, and concentrated to 5.0 mL, yielding MIP-NGs solution. As a reference NG, nonimprinted polymer NGs (NIP-NGs) were prepared by an identical procedure of MIP-NGs without adding HSA.

PIM of NGs for the Introduction of Fluorescent Dye: ATTO 647 N NHS ester (5 mg) was dissolved in DMSO (100 μL). The solution (5 μL) was added to MIP-NGs solution (466 μg/mL, 1 mL) and incubated for 2 h at 25 °C. After the reaction, the mixture was washed by PBS via ultrafiltration (25 °C, 7500 g, 20 min × 3) using a centrifugal filter unit (Amicon Ultra 4–10 kDa), yielding FL-MIP-NGs.

Binding Experiments by SPR Measurements: The SPR sensor chip was washed with EtOH and placed in UV–O_3 for 20 min. The SPR sensor chip was immersed in 1 mM 11-mercaptoundecanoic acid ethanolic solution for 24 h at 25 °C. Subsequently, the chip was washed with EtOH and pure water and dried by N_2 blow. Biacore 3000 instruments were used for NG immobilization. The mixture of 0.4 M EDC and 0.1 M NHS aqueous solutions (1/1, v/v) was injected for activating carboxylic acid on the surface (20 μL min^{-1}, 7 min). Then, NG (MIP-NGs, NIP-NGs, or FL-MIP-NGs) solution was injected (20 μL min^{-1}, 7 min) and the remaining activated carboxylic acids on the chip were inactivated by injecting 1 M amino ethanol (20 μL min^{-1}, 7 min).

Sample proteins (HSA, Trf, Cyt) were dissolved in 10 mM phosphate buffer (pH 7.4, 140 mM NaCl). *RU* values were monitored using 10 mM phosphate buffer (pH 7.4, 140 mM NaCl) as a running buffer, and a sample protein solution (final concentration: 0, 1.5, 3.0, 6.0, 12, 24, 48, 96, 192 nM) was injected with a flow rate of 20 μL min^{-1} and injection volume of 100 μL. The data collection point occurred 6 min after the injection. A difference of bound amounts between substrates was corrected by dividing ΔRU values of protein injection by ΔRU values of NG immobilization.

Binding Experiments by an Autopipetting System Equipped with a Fluorescent Microscope: To investigate the fluorescent signaling abilities of prepared FL-MIP-NGs, the NGs were immobilized on the gold-coated glass substrate (4.3 × 9.8 mm) by same procedure in the case of the SPR sensor chip. The plastic pipette tip was set an NGs-immobilized substrate, and the tip was set at the tip rack.

The NGs-immobilized substrate was incubated in a sample protein solution (0, 12, 24, 48, 96, 192 nM in 10 mM phosphate buffer, pH 7.4 containing 140 mM NaCl, 150 μL) for 10 min at 25 °C. Afterward, the fluorescent intensity was measured at the detection port. Five different ROIs were obtained to calculate the fluorescence intensity of each sensor chip. F_0 and F were fluorescent intensities derived from NGs before and after incubation with proteins, respectively. The light of the mercury lamp passed through a band-pass filter (628 ± 20 nm), and fluorescence was measured using a fluorescent microscope (Zyla 5.5 sCMOS camera, Andor Technology, UK) with a filter (692 nm ± 20 nm).

Binding Constants: Binding constants were estimated by curve-fitting software (DeltaGraph, Nihon Poladigital, Tokyo, Japan). The fitting Equation (1) or (2), which is generally used for determining the binding constant of the formation of a 1:1 complex, is shown. K is the apparent affinity constant ($K_a = 1/K_d$), H is the host, G is the guest, and ΔRU_{max} and ΔF_{max} are the ΔRU and ΔF values given by the binding at the maximum amount of guests found by fitting a theoretical curve to the raw data. Equation (1) and (2) are used for the curve fitting to obtain the SPR and fluorescent detection, respectively.

$$\Delta RU = \Delta RU_{max} \times \frac{1 + K[G] + K[H] - \sqrt{(1 + K[G] + K[H])^2 - 4K^2[G][H]}}{2K[H]} \tag{1}$$

$$\frac{\Delta F}{F_0} = \frac{\Delta F_{max}}{F_0} \times \frac{1 + K[G] + K[H] - \sqrt{(1 + K[G] + K[H])^2 - 4K^2[G][H]}}{2K[H]} \tag{2}$$

© 2021 The Authors. Advanced NanoBiomed Research published by Wiley-VCH GmbH

The apparent limit of detection for the HSA was estimated from the binding isotherm using 3SD/*m* (*m*: the slope of the linear region of the binding isotherm and SD: standard deviation for 0 ng mL^{-1} HSA).

Statistical Analysis: In the SPR measurements, each experiment was conducted in quadruple to calculate an average and a standard deviation. *T*-tests were conducted assess significant differences in the selectivity. In the fluorescent detection, the measurements were carried out in triplicate in the five region of interests (ROIs) with a software equipped with a fluorescent microscope (Andor SOLIS ver. 4.23., Andor Technology Ltd, Belfast, UK).

Supporting Information

Supporting Information is available from the Wiley Online Library or from the author.

Acknowledgements

The authors thank Dr. Sachiko Inubushi (Kobe University) for her kind assistance on the preparation of documents submitted to the Institutional Review Board in Kobe University Hospital. This work was partially supported by Japan Society for the Promotion of Science (JSPS) KAKENHI grant numbers JP16K18300 and JP18H05398 and the Cooperative Research Program of "Network Joint Research Center for Materials and Devices." This work was also partially supported by Japan Agency for Medical Research and Development (AMED) under grant number 19hm0102065h0002. The authors thank the late Professor Isao Karube, President at Tokyo University of Technology (Japan), for his valuable suggestions.

Conflict of Interest

The authors declare no conflict of interest.

Data Availability Statement

Research data are not shared.

Keywords

biosensing, fluorescent sensing, molecular imprinting, polymer nanogels, postimprinting modifications

Received: November 13, 2020
Revised: January 8, 2021
Published online: February 8, 2021

[1] H. J. Lee, E. B. Ehlerding, W. Cai, *Chembiochem* **2019**, *20*, 422.
[2] A. C. Chan, P. J. Carter, *Nat. Rev. Immunol.* **2010**, *10*, 301.
[3] L. M. Weiner, R. Surana, S. Wang, *Nat. Rev. Immunol.* **2010**, *10*, 317.
[4] G. Farahavar, S. S. Abolmaali, N. Gholijani, F. Nejatollahi, *Biomater. Sci.* **2019**, *7*, 4000.
[5] A. Groβ, C. Hashimoto, H. Sticht, J. Eichler, *Front. Bioeng. Biotech.* **2016**, *3*, 211.
[6] M. Famulok, J. S. Hartig, G. Mayer, *Chem. Rev.* **2007**, *107*, 3715.
[7] M. R. Dunn, R. M. Jimenez, J. C. Chaput, *Nat. Rev. Chem.* **2017**, *1*, 0076.
[8] W. Chen, X. Tian, W. He, J. Li, Y. Feng, G. Pan, *BMC Mater.* **2020**, *2*, 1.
[9] K. Ariga, H. Ito, J. P. Hill, H. Tsukube, *Chem. Soc. Rev.* **2012**, *41*, 5800.
[10] M. Komiyama, T. Mori, K. Ariga, *Bull. Chem. Soc. Jpn.* **2018**, *91*, 1075.
[11] T. Takeuchi, T. Hayashi, S. Ichikawa, A. Kaji, M. Masui, H. Matsumoto, R. Sasao, *Chromatography* **2016**, *37*, 43.
[12] T. Takeuchi, T. Mukawa, H. Shinmori, *Chem. Rec.* **2005**, *5*, 263.
[13] J. J. BelBruno, *Chem. Rev.* **2019**, *119*, 94.
[14] H. Taguchi, H. Sunayama, E. Takano, Y. Kitayama, T. Takeuchi, *Analyst* **2015**, *140*, 1448.
[15] X. Ding, P. A. Heiden, *Macromol. Mater. Eng.* **2014**, *299*, 268.
[16] N. Suda, H. Sunayama, Y. Kitayama, Y. Kamon, T. Takeuchi, *R. Soc. Open Sci.* **2017**, *4*, 170300.
[17] T. Saeki, H. Sunayama, Y. Kitayama, T. Takeuchi, *Langmuir* **2019**, *35*, 1320.
[18] Z. Liu, H. He, *Acc. Chem. Res.* **2017**, *50*, 2185.
[19] Y. Inoue, A. Kuwahara, K. Ohmori, H. Sunayama, T. Ooya, T. Takeuchi, *Biosens. Bioelectron.* **2013**, *48*, 113.
[20] W. Wan, M. Biyikal, R. Wagner, B. Sellergren, K. Rurack, *Angew. Chem. Int. Ed.* **2013**, *52*, 7023.
[21] C. Gomy, A. R. Schmitzer, *Org. Lett.* **2007**, *9*, 3865.
[22] N. Murase, T. Mukawa, H. Sunayama, T. Takeuchi, *J. Polym. Sci. B: Polym. Phys.* **2016**, *54*, 1637.
[23] F. Mirata, M. Resmini, in *Molecularly Imprinted Polymers in Biotechnology* (Eds: B. Mattiasson, L. Ye), Springer International Publishing, Cham **2015**, p. 107.
[24] G. Wulff, J. Liu, *Acc. Chem. Res.* **2012**, *45*, 239.
[25] T. Takeuchi, H. Sunayama, *Chem. Commun.* **2018**, *54*, 6243.
[26] K. Takeda, A. Kuwahara, K. Ohmori, T. Takeuchi, *J. Am. Chem. Soc.* **2009**, *131*, 8833.
[27] T. Takeuchi, T. Mori, A. Kuwahara, T. Ohta, A. Oshita, H. Sunayama, Y. Kitayama, T. Ooya, *Angew. Chem. Int. Ed.* **2014**, *53*, 12765.
[28] H. Sunayama, Y. Kitayama, T. Takeuchi, *J. Mol. Recognit.* **2018**, *31*, e2633.
[29] R. Horikawa, H. Sunayama, Y. Kitayama, E. Takano, T. Takeuchi, *Angew. Chem. Int. Ed.* **2016**, *55*, 13023.
[30] T. Morishige, E. Takano, H. Sunayama, Y. Kitayama, T. Takeuchi, *ChemNanoMat* **2019**, *5*, 224.
[31] H. Sunayama, T. Ohta, A. Kuwahara, T. Takeuchi, *J. Mater. Chem. B* **2016**, *4*, 7138.
[32] B. R. Smith, S. S. Gambhir, *Chem. Rev.* **2017**, *117*, 901.
[33] T. Takeuchi, Y. Kitayama, R. Sasao, T. Yamada, K. Toh, Y. Matsumoto, K. Kataoka, *Angew. Chem. Int. Ed.* **2017**, *56*, 7088.
[34] K. Haupt, P. X. Medina Rangel, B. T. S. Bui, *Chem. Rev.* **2020**, *120*, 9554.
[35] H. Sunayama, T. Ooya, T. Takeuchi, *Chem. Commun.* **2014**, *50*, 1347.
[36] G. J. Quinlan, G. S. Martin, T. W. Evans, *Hepatology* **2005**, *41*, 1211.
[37] S. Choi, E. Y. Choi, D. J. Kim, J. H. Kim, T. S. Kim, S. W. Oh, *Clin. Chim. Acta* **2004**, *339*, 147.
[38] J. T. Peters, *All About Albumin: Biochemistry, Genetics, and Medical Applications*, Elsevier Inc. Philadelphia, PA **1995**.
[39] K. Ishihara, *J. Biomed. Mater. Res. A* **2019**, *107*, 933.
[40] J. Ghuman, P. A. Zunszain, I. Petitpas, A. A. Bhattacharya, M. Otagiri, S. Curry, *J. Mol. Biol.* **2005**, *353*, 38.
[41] E. Takano, N. Shimura, T. Akiba, Y. Kitayama, H. Sunayama, K. Abe, K. Ikebukuro, T. Takeuchi, *Microchim. Acta* **2017**, *184*, 1595.
[42] E. Takano, N. Shimura, Y. Ujima, H. Sunayama, Y. Kitayama, T. Takeuchi, *ACS Omega* **2019**, *4*, 1487.
[43] R. E. Wang, L. Tian, Y.-H. Chang, *J. Pharm. Biomed. Anal.* **2012**, *63*, 165.
[44] H.-Y. Lin, M.-S. Ho, M.-H. Lee, *Biosens. Bioelectron.* **2009**, *25*, 579.
[45] Y.-Z. Wang, D.-Y. Li, X.-W. He, W.-Y. Li, Y.-K. Zhang, *Microchim. Acta* **2015**, *182*, 1465.
[46] H. Matsumoto, H. Sunayama, Y. Kitayama, E. Takano, T. Takeuchi, *Sci. Tech. Adv. Mater.* **2019**, *20*, 305.
[47] H. Sunayama, T. Ooya, T. Takeuchi, *Biosens. Bioelectron.* **2010**, *26*, 458.
[48] T. Takeuchi, K. Mori, H. Sunayama, E. Takano, Y. Kitayama, T. Shimizu, Y. Hirose, S. Inubushi, R. Sasaki, H. Tanino, *J. Am. Chem. Soc.* **2020**, *142*, 6617.

 © 2021 The Authors. Advanced NanoBiomed Research published by Wiley-VCH GmbH